Optical and Quantum Electronics (2024) 56:1219
https://doi.org/10.1007/s11082-024-06868-9

Design and analysis of high performance 1×N optical wavelength demultiplexers based on MIM waveguide with polygon resonators

Semih Korkmaz[1]

Received: 7 December 2023 / Accepted: 18 March 2024 / Published online: 19 June 2024

Abstract
Confinement of the light at the subwavelength scale makes photonic devices more efficient in applications such as optical filtering, switching, and sensing with their low dimensions. Metal-insulator- metal waveguide-based configurations present many paths for manipulating light at the wide range of the electromagnetic spectrum. For that purpose, in this study, a wavelength demultiplexer (WDM) based on a metal-insulator-metal (MIM) waveguide is numerically investigated by finite difference time domain (FDTD) method. Proposed WDMs have cascade polygon resonators. After optimizing the fundamental filter, this structure is formed as 1×N demultiplexers. The proposed demultiplexers have two- and three channels. The minimum full width at half-maximum (FWHM) value for these channels is 20.02 nm and the maximum quality factor value is 47.7 at 954.9 nm wavelength. The minimum crosstalk value is obtained as -30.37 dB for this study. The proposed 1×N demultiplexers have potential tools to design low-cost integrated optical circuits for specific wavelengths.

Keywords Waveguides · Demultiplexers · Optical circuits · Resonators · Filters · Crosstalk

1 Introduction

Optical signals are used to transmit data across distances. During this transmission, certain interferences may cause distortions in the signal (Chartier 2005). Optical devices exhibit sufficient transmission performance to reduce these effects and enable reliable data transmission to multiple points simultaneously (Murphy 2020). Techniques such as wavelength division multiplexing and demultiplexing have paved the way to effectively provide the capacity of optical devices (Hu et al. 2011; Zhang et al. 2017; Si and Cheng 2003). The

✉ Semih Korkmaz
semihkorkmaz@bandirma.edu.tr

[1] Department of Computer Engineering, Bandirma Onyedi Eylul University, Balikesir 10200, Turkey

increasing interest in integrated optical circuits for high-speed signal processing has diversified the efforts to improve their performance (Khonina et al. 2022). The most important performance parameters in optical devices for specific wavelengths are narrow bandwidth, high-quality factor, and optically tunability (Heydari et al. 2017; Ji et al. 2021; Ma et al. 2021). Confinement of optical signals at specific wavelengths can be easily achieved using surface plasmons (Brongersma and Kik 2007). Surface plasmon polaritons propagate along the waveguides and are confined to specific wavelengths (Oulton et al. 2008). Controlling the light at certain wavelengths in optical ways such as waveguides has formed the basis of many studies. Band-pass and band-stop filtering performance determine the quality of the applications (Cui et al. 2023; Janfaza et al. 2019; Korani et al. 2023; Ebadi et al. 2020; Pinton et al. 2018; Mao et al. 2017). There are many waveguide-based studies such as Mach-Zehnder interferometers (Swarnakar et al. 2021; Yang et al. 2022), modulators (Han et al. 2022; Edelstein et al. 2022), logic devices (Yang et al. 2017; El Haffar et al. 2022; Sreevani et al. 2022; Swarnakar et al. 2023), demultiplexers (Mohammadi et al. 2023; Butt et al. 2023), Bragg reflectors (Zeng et al. 2022; Pallavi et al. 2023), sensors (Bensalah et al. 2022; Bahri et al. 2022; Lai et al. 2018; Salah et al. 2021; Salah et al. 2022) and directional couplers (Nanda et al. 2022; Zhang et al. 2020). The optical demultiplexer is based on the band-pass filter with its optimized parameters such as type and length of resonators. In literature, different shapes of resonators such as disks, rings, rectangles, and hexagons have been used to design optical demultiplexers (Zafar et al. 2019; Khani et al. 2018, 2021; Xie et al. 2016).

In this study, 1×N demultiplexers are proposed based on metal-insulator-metal waveguide including polygon nanostructures. Numerical calculations are done via the commercial Lumerical FDTD solution software (Lumerical 2023). In the first step of this study, a band-pass filter is designed and analyzed via parameter sweep to obtain maximum transmission values at the resonance wavelengths. After determining the geometrical parameters for the proposed band-pass filter can be called one channel-demultiplexer, the number of the channels is increased to design 1×2 and 1×3 optical wavelength demultiplexers. Then, the field distributions are visualized and the transmission, crosstalk, quality factor, and FWHM values are calculated at the resonance wavelengths. Crosstalk and quality factor values determine the efficiency of the demultiplexer. The maximum transmission is 76%, the highest quality factor is 47.7 and the lowest full width at half-maximum (FWHM) value is 20.02 for this study. The minimum crosstalk is -30.37 dB.

2 Design and analysis method

Figure 1 shows a view of the basic filter design. The designed filter has a waveguide with a 50 nm width (w) in three regions and two polygon resonators on a silver layer. The two polygon resonators are etched on the way of the waveguide. The device parameters are L_1=600 nm, L_2=160 nm, L_3=550 nm, L_4=480 nm, L_5=450 nm, d_1=10 nm, w=50 nm. w value is valid for the input, middle, and output parts of the waveguide. The lengths of the band-pass filter are 2.8 μm and 1 μm for the x- and y-axis, respectively. The transmission spectrum of the basic filter design is numerically attained with a 2D-FDTD method. The height of the designed structure in the third dimension is wider than the feature size in the 2D computation plane. Therefore, the effect of the thickness of the substrate on the obtained results is negligible during numerical analysis on the assumption that the structure

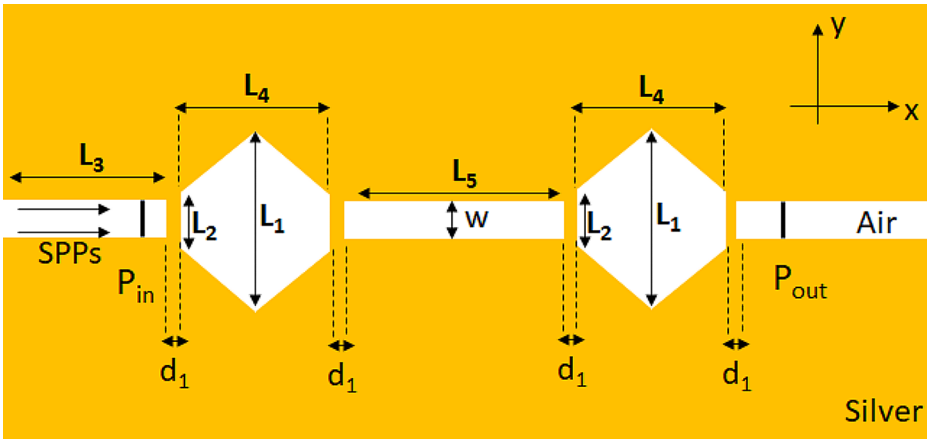

Fig. 1 The view of the basic filter

is infinite in the third dimension (Hocini et al. 2019; Chao et al. 2021). Perfectly matched layer boundary conditions are utilized for x and y-axes during numerical calculations. The simulation region is set as the x- and y-axis length of the structures. The mesh step is set as $\Delta x = \Delta y = 4$ nm. The simulation time is 1000 fs. The orange and white areas in the filter are silver and air, respectively. The optical parameters of silver are taken from Johnson and Christy (Johnson and Christy 1972). As given in Fig. 1, surface plasmon polaritons (SPPs) propagate by transverse magnetic (TM) polarized Gaussian light source along the design. P_{in} and P_{out} values are calculated as input and output power, respectively. The transmission value of the basic filter is calculated via Eq. (1) (Han et al. 2020).

$$T = P_{out}/P_{in} \tag{1}$$

The resonance wavelength of the polygon resonators can be obtained by Eq. (2) (Hocini et al. 2020).

$$\lambda_m = \frac{2Re\left(n_{eff}\right) L_{eff}}{m}, m = 1,2,3,\ldots. \tag{2}$$

where, $Re(n_{eff})$ is the real part of the effective refractive index of the SPP, L_{eff} is the effective resonance length of the resonator and m is the mode number.

The resonance peak occurs at 954.9 nm with a transmission of 76% in Fig. 2(a). The basic filter shows the band-pass filter behavior. The FWHM value is 46.11 and the quality factor value is obtained as 20.71.

The quality factor is calculated with the formula of (3) (Zafar et al. 2019).

$$Q = \lambda res/FWHM \tag{3}$$

The magnetic near-field distribution ($|H|^2/|H_{in}|^2$) at the resonant wavelength is illustrated in Fig. 2(b). The transmitted energy is confined at the edge of the two polygon resonators.

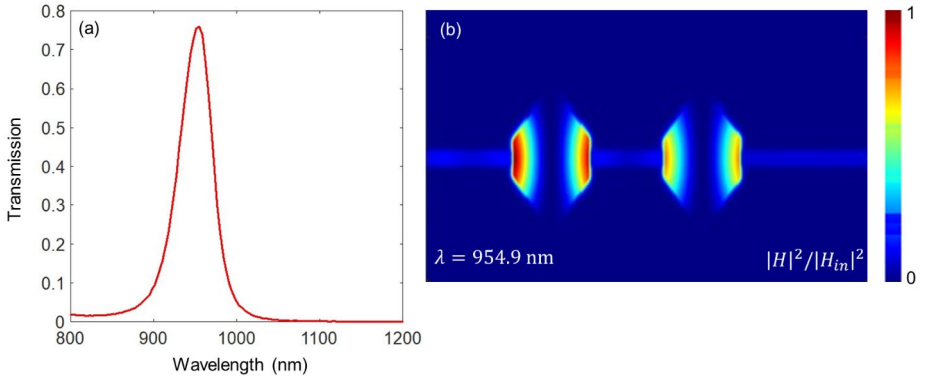

Fig. 2 (**a**) The transmission spectrum of the proposed filter. (**b**) Magnetic near-field distribution at λ=954.9 nm. Corresponding device parameters are L_1=600 nm, L_2=160 nm, L_3=550 nm, L_4=480 nm, L_5=450 nm, d_1=10 nm and w=50 nm

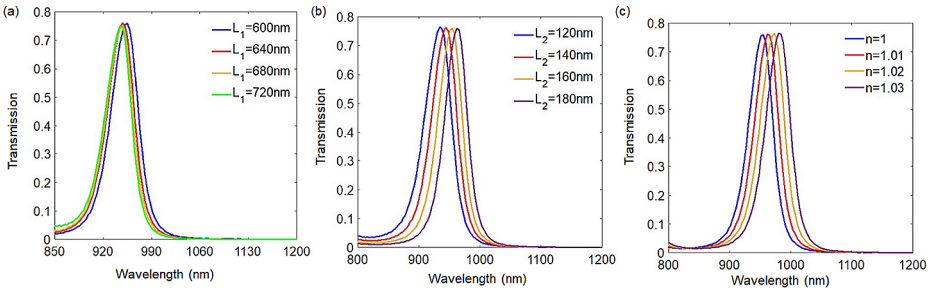

Fig. 3 Parameter sweep for the proposed filter. The transmission spectra of the structure for different values (**a**) L_1, (**b**) L_2, and (**c**) refractive index of the medium (n_{Air}=1). Corresponding device parameters are L_1=600 nm, L_2=160 nm, L_3=550 nm, L_4=480 nm, L_5=450 nm, d_1=10 nm and w=50 nm

The parameter sensitivity performance is important to design demultiplexers with different resonance wavelengths. For that reason, geometrical parameter analysis is done to overcome this performance. While fixing all parameters, only one length value is changed. In Fig. 3(a), L_1 is varied from 600 nm to 720 nm with a 40 nm step size. When L_1 values are increased, the transmission values do not significantly change. In Fig. 3(b), L_2 is changed from 120 nm to 180 nm with a 20 nm step size. When L_2 values are increased, the transmission values prominently shift to higher resonance wavelengths. Although the step size of L_2 is half of the L_1 sweep, significant shifts can be obtained. Since the L_2 part of the polygon resonator meets the TM polarized light at first, L_2 is more critical than L_1 in determining the resonance wavelengths. So, while designing 1×2 and 1×3 demultiplexers, only L_2 values are changed. Figure 3(c) shows the refractive index change in the transmission spectra. As the refractive index values are varied by 1%, shifted resonance values can be obtained without losing transmission values. This behavior shows that the designed demultiplexers can work in different media with significant performance.

3 Results and analyses

Figure 4(a) shows the view of the 1×2 demultiplexer. This demultiplexer has two channels. The distance (L_z) between these channels is 1760 nm. The device parameters are L_1=600 nm, L_3=550 nm, L_4=480 nm, L_5=450 nm, d_1=10 nm, w=50 nm. The other parameters are L_x = 180 nm and L_y = 140 nm. The dimensions of the 1×2 demultiplexer are 2.8 μm and 2 μm for the x- and y-axis, respectively. As discussed in Sect. 2, the L_2 sweep provides district resonance wavelengths. For that purpose, while designing the 1×2 demultiplexer, only the L_2 value is changed. Since there are two channels, L_2 is named L_x and L_y for channel 1 and channel 2, respectively. Figure 4(b) visualizes the transmission spectra of the 1×2 demultiplexer. The transmission values are obtained 65% at 969.3 nm and 67% at 944.4 nm for channel 1 and channel 2, respectively. The FWHM values are 22.46 nm and 28.89 nm and the quality factor values are attained as 43.15 and 32.69 at 969.3 nm and 944.4 nm, respectively. The average FWHM and quality factor values are 25.68 nm and 37.92, respectively. The magnetic near-field distributions on the channels at 969.3 nm and 944.4 nm are visualized in Fig. 4(c) and Fig. 4(d), respectively. Another important parameter is crosstalk values for demultiplexers. Crosstalk, measured in decibels (dB), represents the effect of adjacent channels on the designated channel when an optical wave is sent to the demultiplexer input (Abderrahmane et al. 2023). Table 1 shows the crosstalk values of the 1×2 demultiplexer. The crosstalk is calculated by the formula given below as (4).

$$\text{Crosstalk} = 10 \times \log\left(P_i/P_j\right) \tag{4}$$

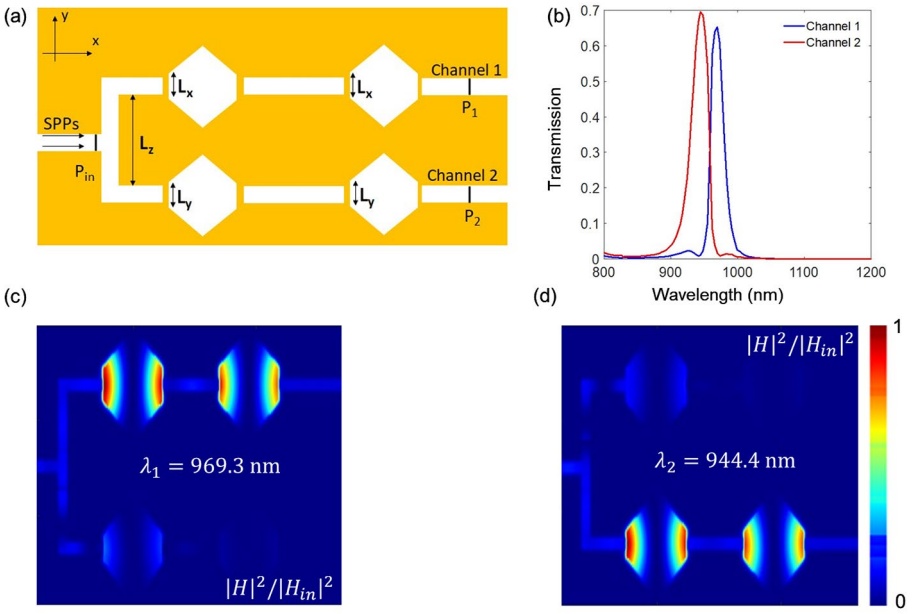

Fig. 4 (**a**) The view of the proposed two-channel demultiplexer with two polygon resonators. (**b**) The transmission spectra of the 1×2 demultiplexer. Magnetic near-field distributions at (**c**) λ_1=969.3 nm and (**d**) λ_2=944.4 nm. Corresponding device parameters are L_1=600 nm, L_x = 180 nm, L_y = 140 nm, L_z = 1760 nm L_3=550 nm, L_4=480 nm, L_5=450 nm, d_1=10 nm and w=50 nm

Table 1 Crosstalk values at the corresponding resonance wavelengths of the proposed 1×2 demultiplexer

Crosstalk(dB)	Channel 1	Channel 2
Channel 1	…….	-15.79
Channel 2	-18.05	…….

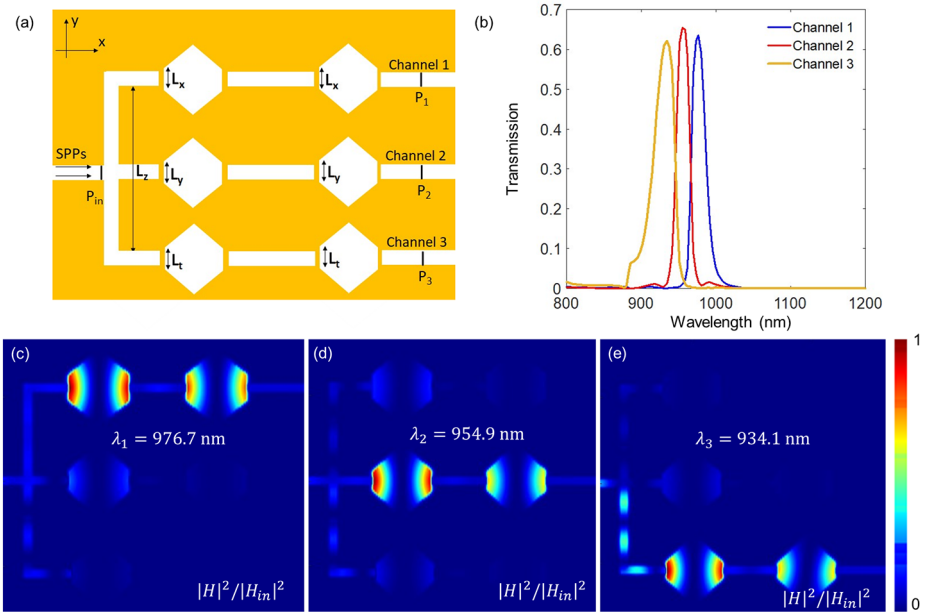

Fig. 5 (**a**) The view of the designed three-channel demultiplexer with two polygon resonators. (**b**) The transmission spectra of the 1×3 demultiplexer. Magnetic near-field distributions at (**c**) λ_1=976.7 nm, (**d**) λ_2=954.9 nm, and (**e**) λ_3=934.1 nm. Corresponding device parameters are L_1=600 nm, L_x = 200 nm, L_y = 160 nm, L_t = 120 nm, L_z = 2120 nm, L_3=550 nm, L_4=480 nm, L_5=450 nm, d_1=10 nm and w=50 nm

where *i* and *j* are channel's number (Moradiani et al. 2020).

Figure 5(a) shows the view of the 1×3 demultiplexer. This demultiplexer has three channels. The distance (L_z) between channel 1 and channel 3 is 2120 nm. Channel 2 is located in the middle of the other channels. The device parameters are L_1=600 nm, L_3=550 nm, L_4=480 nm, L_5=450 nm, d_1=10 nm, w=50 nm. The other parameters are L_x = 200 nm, L_y = 160 nm, L_t = 120 nm. The lengths of the 1×3 demultiplexer are 2.8 µm and 3 µm for the x- and y-axis, respectively. Since there are three channels, L_2 is named L_x, L_y, and L_t for channel 1, channel 2, and channel 3, respectively. Figure 5(b) presents the transmission spectra of the 1×3 demultiplexer. The transmission values are obtained as 64% at 976.7 nm, 66% at 954.9 nm, and 62% at 934.1 nm for channel 1, channel 2, and channel 3, respectively. The FWHM values are 20.92 nm, 20.02 nm, and 31.14 nm and the quality factor values are obtained as 46.69, 47.7, and 30 at 976.7 nm, 954.9 nm, and 934.1 nm, respectively. The average FWHM and quality factor values are 24.02 nm and 41.46, respectively. The magnetic near-field distributions on the channels at 976.7 nm, 954.9 nm, and 934.1 nm are seen in Fig. 5(c), Fig. 5(d), and Fig. 5(e) respectively. Table 2 shows the crosstalk values of 1×3 demultiplexer. When comparing the FWHM and quality factor values among

Table 2 Crosstalk values at the corresponding resonance wavelengths of the proposed 1×3 demultiplexer

Crosstalk (dB)	Channel 1	Channel 2	Channel 3
Channel 1	……	-15.65	-29.76
Channel 2	-17.91	…….	-13.58
Channel 3	-30.37	-17.07	…….

Table 3 Comparisons between the proposed demultiplexers and other studies

Ref.	Number of channels	Maximum transmission	Minimum FWHM (nm)	Maximum quality factor	Minimum crosstalk (dB)
(Zafar et al. 2019)	2	45	–	60	-30
(Khani et al. 2018)	3	50	36	38.11	–
(Khani et al. 2021)	2	56.7	32.56	33	–
	4	54.13	83.1	16.57	–
(Abbaszadeh-Azar and Abedi 2020)	4	40	60	–	–
(Asgari and Fabritius 2020)	2	55	220	–	-48.3
(Han et al. 2020)	4	68	37	–	-13.7
(Xie et al. 2016)	3	50.95	28.4	–	–
(Azzazi and Swillam 2015)	4	52	9.8	–	–
(Faghani et al. 2021)	3	80	–	–	-23
(Truong et al. 2021)	3	30	90	–	-15
This work	*2*	*65*	*22.46*	*43.15*	*-18.05*
This work	*3*	*66*	*20.02*	*47.7*	*-30.37*

the band-pass filter (1×1), 1×2, and 1×3 demultiplexers, it is observed that the FWHM values decrease while the quality factor values increase. When the number of channels is increased, the coupling strength between the polygon resonators on the different channels is increased resulting in narrower FWHM and higher quality factor (Khani et al. 2021). This trend indicates an enhancement in device performance. In addition to this, 1×1, 1×2 and 1×3 demultiplexers have different dimensions such as 2.8 μm^2, 5.6 μm^2, and 8.4 μm^2, respectively. However, the maximum transmission loss is at around 15% as compared with the designed demultiplexers. To demonstrate the efficiency of the designed demultiplexers, the transmission, FWHM, quality factor, and crosstalk values in this study are compared with those reported in prior work, as presented in Table 3. When these values are compared with previously reported studies, it is seen that this study has better performance values in designing optical wavelength demultiplexers.

4 Conclusion

In this study, 1×N demultiplexers have been numerically designed and analyzed by the FDTD method. The two and three-channel demultiplexers have been proposed based on a single-mode band pass-filter including two similar polygon resonators. Thanks to high geometrical parameter sensitivity, discrete resonances have been obtained and the wavelength demultiplexers have been designed. The highest transmission and quality factor values of this study are 76% and 47.7 nm, respectively. The minimum FWHM is 20.02 nm. The lowest crosstalk value is obtained as -30.37 dB. The results show that increasing the

number of channels supports the lower FWHM and crosstalk values and higher quality factors which are indispensable for optical devices. The lowest distance is 10 nm between the polygon resonators and the straight waveguides. When the proposed structure is also thought for experimental study, it can be achieved via the last nanofabrication techniques without transmission loss as given in the geometric parameter sweep analyses. Highly efficient performances support better transmission, quality factor, FWHM, and crosstalk values as compared with the literature. The proposed demultiplexers exhibit a wide range of applications within the concept of highly integrated optical circuits via their appropriately sized configurations.

Author contributions S.K. prepared the figures and tables and wrote the main manuscript text.

Funding Open access funding provided by the Scientific and Technological Research Council of Türkiye (TÜBİTAK).

Data availability No datasets were generated or analysed during the current study.

Declarations

Competing interests The authors declare no competing interests.

References

Abbaszadeh-Azar, O., Abedi, K.: A wavelength demultiplexing structure based on the multi-teeth-shaped plasmonic waveguide structure. Plasmonics. **15**, 1403–1409 (2020)

Abderrahmane, I., Hadjira, B., Mehadji, A.: Efficient 4 and 8 plasmonic wavelength DEMUX with Ultra high Q-factor and low FWHM based on nano-rectangular resonators. Opt. Quantum Electron. **55**(2), 108 (2023)

Asgari, S., Fabritius, T.: Tunable mid-infrared graphene plasmonic cross-shaped resonator for demultiplexing application. Appl. Sci. **10**(3), 1193 (2020)

Azzazi, A., Swillam, M.A.: Nanoscale highly selective plasmonic quad wavelength demultiplexer based on a metal–insulator–metal. Opt. Commun. **344**, 106–112 (2015)

Bahri, H., Hocini, A., Bensalah, H., Mouetsi, S., Ingebrandt, S., Pachauri, V., Hamani, M.: A high-sensitivity biosensor based on a metal–insulator–metal diamond resonator and application for biochemical and environment detections. Optik. **271**, 170083 (2022)

Bensalah, H., Hocini, A., Bahri, H.: Design and analysis of a mid-infrared ultra-high sensitive sensor based on metal-insulator-metal structure and its application for temperature and detection of glucose. Prog Electromagn. Res. M 112 (2022)

Brongersma, M.L., Kik, P.G.: Surface Plasmon Nanophotonics. Springer, The Netherlands (2007)

Butt, M.A., Kazanskiy, N.L., Khonina, S.N.: Miniaturized design of a 1× 2 plasmonic demultiplexer based on metal–insulator-metal waveguide for telecommunication wavelengths. Plasmonics. **18**(2), 635–641 (2023)

Chao, C.T.C., Chau, Y.F.C., Chiang, H.P.: Multiple Fano resonance modes in an ultra-compact plasmonic waveguide-cavity system for sensing applications. Results Phys. **27**, 104527 (2021)

Chartier, G.: Introduction to Optics. Springer, New York (2005)
Cui, P., Huo, Y., Zhang, Z., Wang, Y., Song, M., Zhao, C., Liu, T., Liao, Z.: Band-stop filter and narrow band-pass filter based on metal-insulator-metal waveguide. Micro Nanostruct. **175**, 207503 (2023)
Ebadi, S.M., Örtegren, J., Bayati, M.S., Ram, S.B.: A multipurpose and highly-compact plasmonic filter based on metal-insulator-metal waveguides. IEEE Photonics J. **12**(3), 1–9 (2020)
Edelstein, S., Indukuri, S.C., Mazurski, N., Levy, U.: Waveguide-integrated mid-IR photodetector and all-optical modulator based on interlayer excitons absorption in a WS2/HfS2 heterostructure. Nanophotonics. **11**(19), 4337–4345 (2022)
El Haffar, R., Mahboub, O., Farkhsi, A., Figuigue, M.: All-optical logic gates using a plasmonic MIM waveguide and elliptical ring resonator. Plasmonics 1–12 (2022)
Faghani, A.A., Yaghoubi, E., Yaghoubi, E.: Triple-channel glasses-shape nanoplasmonic demultiplexer based on multi nanodisk resonators in MIM waveguide. Optik. **237**, 166697 (2021)
Han, J., Huang, J., Wu, J., Yang, J.: Inverse-designed tunable four-channel wavelength demultiplexer. Opt. Commun. **465**, 125606 (2020)
Han, C., Jin, M., Tao, Y., Shen, B., Wang, X.: Recent progress in silicon-based slow-light electro-optic modulators. Micromachines. **13**(3), 400 (2022)
Heydari, S., Pedram, K., Ahmed, Z., Zarrabi, F.B.: Dual-band monopole antenna based on metamaterial structure with narrowband and UWB resonances with reconfigurable quality. AEU - Int. J. Electron. Commun. **81**, 92–98 (2017)
Hocini, A., Temmar, M.N., Khedrouche, D.: Design of mid-infrared high sensitive metal-insulator-metal plasmonic sensor. Chin. J. Phys. **61**, 86–97 (2019)
Hocini, A., Ben Salah, H., Khedrouche, D., Melouki, N.: A high-sensitive sensor and band-stop filter based on intersected double ring resonators in metal–insulator–metal structure. Opt. Quantum Electron. **52**, 1–10 (2020)
Hu, F., Yi, H., Zhou, Z.: Wavelength demultiplexing structure based on arrayed plasmonic slot cavities. Opt. Lett. **36**(8), 1500–1502 (2011)
Janfaza, M., Mansouri-Birjandi, M.A., Tavousi, A.: Proposal for a graphene nanoribbon assisted mid-infrared band-stop/band-pass filter based on Bragg gratings. Opt. Commun. **440**, 75–82 (2019)
Ji, X., Roberts, S., Corato-Zanarella, M., Lipson, M.: Methods to achieve ultra-high quality factor silicon nitride resonators. APL Photonics **6**(7) (2021)
Johnson, P.B., Christy, R.W.: Optical constants of the noble metals. Phys. Rev. B. **6**(12), 4370 (1972)
Khani, S., Danaie, M., Rezaei, P.: Double and triple-wavelength plasmonic demultiplexers based on improved circular nanodisk resonators. Opt. Eng. **57**(10), 107102–107102 (2018)
Khani, S., Farmani, A., Mir, A.: Reconfigurable and scalable 2, 4-and 6-channel plasmonics demultiplexer utilizing symmetrical rectangular resonators containing silver nano-rod defects with FDTD method. Sci. Rep. **11**(1), 13628 (2021)
Khonina, S.N., Kazanskiy, N.L., Butt, M.A., Karpeev, S.V.: Optical multiplexing techniques and their marriage for on-chip and optical fiber communication: A review. Opto-Electron Adv. **5**(8), 210127–210121 (2022)
Korani, N., Abbasi, A., Danaie, M.: Band-pass and Band-stop Plasmonic Filters based on Wilkinson Power Divider structure. Plasmonics 1–10 (2023)
Lai, W., Wen, K., Lin, J., Guo, Z., Hu, Q., Fang, Y.: Plasmonic filter and sensor based on a subwavelength end-coupled hexagonal resonator. Appl. Opt. **57**(22), 6369–6374 (2018)
Lumerical, F.D.T.D.: Solutions (Finite-Difference-Time-Domain Package) (2023). www.lumerical.com
Ma, Q., Ren, G., Xu, K., Ou, J.Z.: Tunable optical properties of 2D materials and their applications. Adv. Opt. Mater. **9**(2), 2001313 (2021)
Mao, J., Zhai, X., Wang, L., Li, H.: Numerical analysis of near-infrared plasmonic filter with high figure of merit based on Fano resonance. Appl. Phys. Express. **10**(8), 082201 (2017)
Mohammadi, M., Soroosh, M., Farmani, A., Ajabi, S.: Engineered FWHM enhancement in plasmonic nanoresonators for multiplexer/demultiplexer in visible and NIR range. Optik. **274**, 170583 (2023)
Moradiani, F., Mohamadi, A.M., Seifouri, M.: High-performance tunable multi-channel graphene-based square ring resonator demultiplexer. Opt. Commun. **475**, 126218 (2020)
Murphy, E.J.: Integrated Optical Circuits and Components: Design and Applications. CRC, New York (2020)
Nanda, R., Rath, R., Swarnakar, S., Kumar, S.: Design of all-optical directional coupler using plasmonic MIM waveguide for switching applications. Plasmonics. **17**(5), 2153–2159 (2022)
Oulton, R.F., Sorger, V.J., Genov, D.A., Pile, D.F.P., Zhang, X.: A hybrid plasmonic waveguide for subwavelength confinement and long-range propagation. Nat. Photonics. **2**(8), 496–500 (2008)
Pallavi, M., Thipparaju, R.R., Mondal, S., Mohandas, S.: Optimization of strip-based hybrid plasmonic terahertz waveguide with distributed Bragg reflector layers. Opt. Eng. **62**(3), 037108–037108 (2023)

Pinton, N., Grant, J., Collins, S., Cumming, D.R.: Exploitation of magnetic dipole resonances in metal–insulator–metal plasmonic nanostructures to selectively filter visible light. ACS Photonics. **5**(4), 1250–1261 (2018)

Salah, H.B., Hocini, A., Bahri, H., Melouki, N.: High sensitivity plasmonic sensor based on metal–insulator–metal waveguide coupled with a notched hexagonal ring resonator and a stub. ECS J. Solid State Sci. Technol. **10**(8), 081001 (2021)

Salah, H.B., Bahri, H., Hocini, A., Zegaar, I., Ingebrandt, S., Pachauri, V.: Design of a plasmonic sensor based on a nanosized structure for biochemical application. J. Phys. Conf. Ser. **2240**(1), 012024 (2022)

Si, Y.C., Cheng, Y.: Optical multiplexer/demultiplexer: Discrete. WDM Technologies Academic (2003)

Sreevani, A., Charles, I., Swarnakar, S., Krishna, S.V., Kumar, S.: Design and characteristic analysis of an all-optical AND, XOR, and XNOR Y-shaped MIM waveguide for high-speed information processing. Appl. Opt. **61**(5), 1212–1218 (2022)

Swarnakar, S., Reddy, S.K., Harijan, R., Kumar, S.: Design and modeling of all-optical NAND gate using metal–insulator–metal (MIM) waveguides-based Mach–Zehnder interferometers for high-speed information processing. Opt. Quantum Electron. **53**(9), 493 (2021)

Swarnakar, S., Basha, S.C.A., Azmathullah, S., Prabhu, N.A., Madhu, G., Kumar, S.: Improved design of all-optical half-adder and half-subtractor circuits using MIM plasmonic waveguides for optical networks. Opt. Quantum Electron. **55**(1), 94 (2023)

Truong, C.D., Van, T.N., Trinh, M.T., Manh, H.C., Tan, H.N., Hoai, B.D.: Triple-wavelength filter based on the nanoplasmonic metal-insulator-metal waveguides. Opt. Quantum Electron. **53**, 1–15 (2021)

Xie, Y.Y., He, C., Li, J.C., Song, T.T., Zhang, Z.D., Mao, Q.R.: Theoretical investigation of a plasmonic demultiplexer in MIM waveguide crossing with multiple side-coupled hexagonal resonators. IEEE Photonics J. **8**(5), 1–12 (2016)

Yang, X., Hu, X., Yang, H., Gong, Q.: Ultracompact all-optical logic gates based on nonlinear plasmonic nanocavities. Nanophotonics. **6**(1), 365–376 (2017)

Yang, R., Xie, Y.Y., Chai, J.X., Ye, Y.C., Liu, B.C., Jiang, X., Dai, L., Feng, M.Y.: Theoretical investigation of a multi-functional logic device based on plasmonic Mach-Zehnder interferometer waveguides. Opt. Laser Technol. **151**, 108076 (2022)

Zafar, R., Chauhan, P., Salim, M., Singh, G.: Metallic slit–loaded ring resonator–based plasmonic demultiplexer with large crosstalk. Plasmonics. **14**(4), 1013–1017 (2019)

Zeng, L., Li, J., Cao, C., Li, X., Zeng, X., Yu, Q., Wen, K., Yang, J., Qin, Y.: An integrated-plasmonic chip of Bragg reflection and Mach-Zehnder interference based on metal-insulator-metal waveguide. Photonic Sens. **12**(3), 220303 (2022)

Zhang, S., Ji, W., Yin, R., Li, X., Gong, Z., Lv, L.: Full bandwidth wavelength division multiplexer/demultiplexer based on MMI. IEEE Photon Technol. Lett. **30**(1), 107–110 (2017)

Zhang, L., Pan, C., Zeng, D., Yang, Y., Yang, Y., Ma, J.: A hybrid-plasmonic-waveguide-based polarization-independent directional coupler. IEEE Access. **8**, 134268–134275 (2020)